Adaptive secondary mirror demonstrator: construction and preliminary evaluation

Jun Ho Lee*
David D. Walker
A. Peter Doel
University College London
Department of Physics and Astronomy
Optical Sciences Laboratory
Gower Street
London WC1E 6BT
United Kingdom

Abstract. Adaptive optics (AO) combines technologies that enable the correction of the wavefront distortion caused by the earth's atmospheric turbulence in real time. Adaptive secondary mirror (ASM) systems have been proposed and are now being developed. ASMs have advantages over conventional AO systems in terms of throughput, polarization and IR emissivity. Previously, we reported the design of an ASM demonstrator along with its predicted performance. We now report the construction techniques and the results from the preliminary static and dynamic testing of such a demonstrator. In particular, assembly methods that preserve the optical quality of the mirror are presented along with experimentally measured mirror influence functions and closed loop tip/tilt performance.
[S0091-3286(00)00304-4]

Subject terms: adaptive optics; deformable mirror; wavefront corrections; secondary mirror.

Paper 990127 received Mar. 22, 1999; revised manuscript received Sep. 7, 1999; accepted for publication Sep. 10, 1999.

1 Introduction

Adaptive optics systems remove the wavefront distortion introduced by the earth's atmosphere (or other turbulent medium) by introducing a controllable counterwavefront distortion that both spatially and temporally follows that of the atmosphere.[1] Adaptive secondary mirrors (ASMs) were proposed by Beckers.[2] Since the ASM uses an existing optical surface (the secondary mirror), the approach has several advantages compared to the conventional (and often complex) adaptive optics implementation. These advantages are (1) optical throughput is enhanced; (2) negligible extra IR emissivity is introduced, which is a crucial advantage for a system intended to operate primarily in the IR; and (3) no extra polarization is added.

Tip/tilt secondary mirrors were first developed at the Steward Observatory[3] and in a collaboration between the Royal Observatory Edinburgh (ROE) and the Max-Plank Institute für Astronomic Heidelberg (MPIA) (Ref. 4). Currently, deformable secondary mirrors are being developed at the Steward Observatory in collaboration with ThermoTrex,[5] and at the Optical Science Laboratory[6–10] (OSL).

The OSL previously demonstrated the optical efficacy and mechanical feasibility of performing the adaptive correction and IR chopping with an adaptive secondary mirror and proposed a design for a 1 m diameter ASM with 90 actuators compatible with possible future requirements of the Gemini project. Recently, we developed a prototype (or demonstrator) of the 1 m ASM (Fig. 1), the purpose of which is to evaluate features and capabilities applicable to the full-size system.

*Current affiliation: Korea Advanced Institute of Science and Technology, Satellite Research Center, 373-1 Kusong-dong, Yusong-gu, Taejon 305-701, South Korea. E-mail: jhl@satrec.kaist.ac.kr.

The design of the demonstrator together with the finite element analysis (FEA) predicted performance (Fig. 1) was previously presented.[9] This paper describes the construction, assembly techniques and subsequent preliminary static and dynamic performance evaluation. As discussed in the next section, the key considerations in building an ASM are reliability and safety. It is shown that the demonstrator can satisfy the principal requirements.

2 Principal Requirements in Building an ASM

An ASM is an integral part of the telescope rather than an independent instrument. Therefore, the telescope as a system will fail if the ASM control fails. Moreover, when near Zenith-pointing, the secondary mirror is directly over the telescope primary, which is therefore potentially vulnerable to any catastrophic stress-induced fracture of the secondary.

Therefore, there are compelling advantages for ASM systems to use rugged engineering materials not subject to brittleness or stress-induced failure at defects. Certain elements of the control system (particular power supplies, power drivers) may usefully be duplicated to provide redundancy, if this can be made consistent with the allowable mass and mass-moment budgets.

There is also a very strong pointer toward incorporating a switch-off mode, so that the secondary will still provide scientifically useful imaging (even if degraded and/or for use only in the IR) in the event of a complete control-system failure. In the case of a partial failure (e.g., one actuator goes to maximum extent), stresses applied to the mirror substrate should lie at an adequate safety margin below the yield strength.

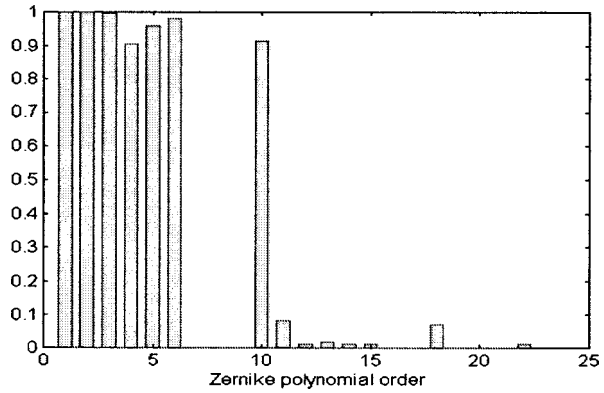

Fig. 1 Ability of the demonstrator to fit Zernike terms. A *z*-axis value of 1 indicates perfect matching, while 0 represents zero ability to fit the term.

3 Construction

3.1 *Design of the Demonstrator*

The design of the demonstrator was presented in the previous paper,[9] as shown in Fig. 2. The 10 mm thick meniscus faceplate has seven tapped blind holes in the back surface to which the actuators are interfaces via flexures. The reaction (or backing) plate provides the resistance to the reaction forces of the actuators, and the interface to the telescope. It is currently a simple plate for laboratory tests and it will eventually be replaced with a light-weight stiff aluminum structure.

An aluminum alloy was chosen as the material for the mirror substrate since it is a ductile material with some 20 times the yield strength of polished glass and 50 times that of ground glass. The yield strength is not reduced by accidental damage, unlike glass or glass ceramics. Therefore, aluminum alloy can achieve the safety margins we require. It can also carry threaded holes for attachment to actuators. The flexures and reaction plate were chosen to be all of the same material to minimize thermal distortion.

3.2 *Faceplate*

The mirror faceplate was machined, ground, thermally cycled, prepolished, electroless nickel plated and repolished using proprietary polishing techniques. The nickel coating

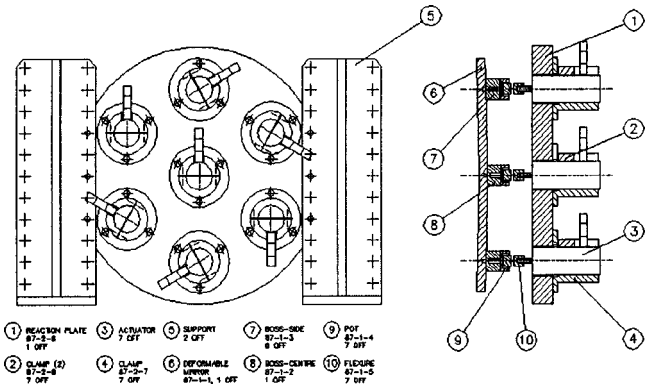

Fig. 2 Mechanical drawing of the assembled demonstrator.

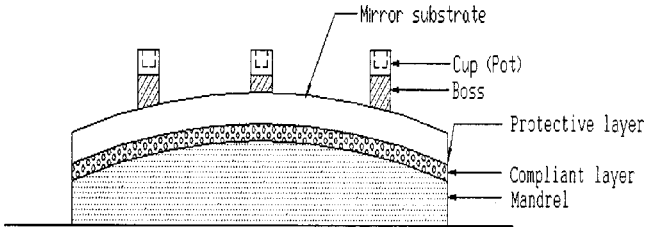

Fig. 3 Schematic diagram of the assembly setup.

of the faceplate was necessary due to the soft nature of aluminum, which will not directly take an optical polish and which can corrode.

3.3 *Actuators and Displacement Sensors*

One of the major drivers in the selection of the actuators used for the demonstrator was their long term reliability. Based on manufacturer's data for stroke, frequency response and service life, which were confirmed independently by our lab testing,[10] magneto-strictive (MS) actuators with a stroke of ± 25 μm were chosen as the positioning devices. A strain gauge was selected as the displacement sensor because it could be easily packaged together with the actuator.

3.4 *Assembly*

The assembly process is one of the key features that the demonstrator project aims to develop. In particular the goal of a switched off mode requires the mirror to keep its optical quality during the assembly process.

During assembly (Fig. 3), the bosses carrying cups were screwed into the rear of the mirror faceplate, using a locking compound to secure them in place. Figure 4 shows a schematic diagram of coupling between the faceplate and an actuator. The mirror faceplate was placed face down on an isolating mandrel, with a compliant layer between, for this operation. The rear system comprising backing plate, actuators, flexures and pistons were then assembled. The following procedure was then implemented to preserve the stress free state of the mirror faceplate while it was attached to the actuators. The rear system was carefully lowered onto the back of the mirror faceplate so that the actuator pistons lay within, but not touching, the cups. The cups were then filled with epoxy, which was then cured to complete the assembly without disturbing the optical surface. By these processes, we achieved the assembly with a

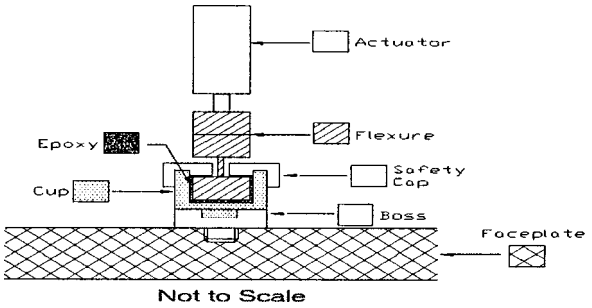

Fig. 4 Schematic diagram of coupling between the faceplate and an actuator.

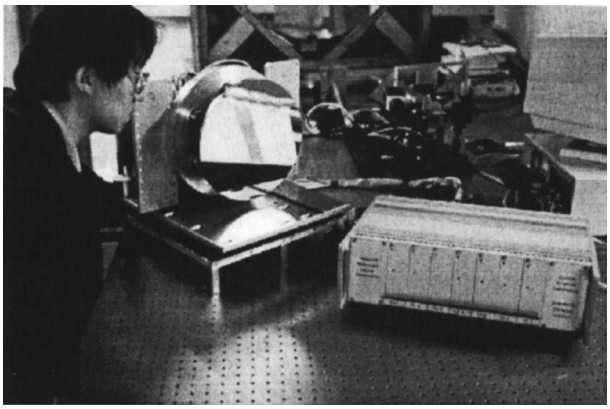

Fig. 5 The demonstrator unit after assembly.

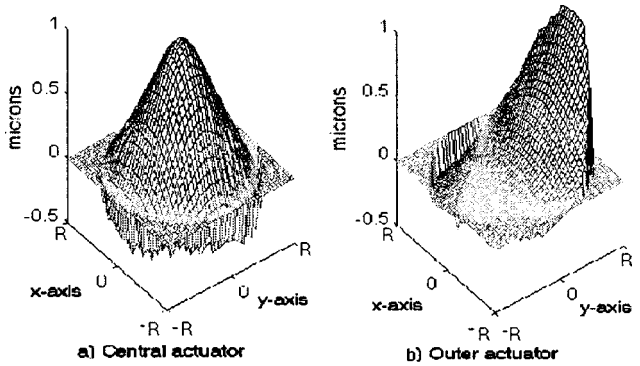

Fig. 6 Measured influence functions of the central and outer actuators. The influence functions are scaled to have a maximum of 1 Om, and *R* is the radius of the mirror.

change in the mirror overall shape of 10 nm root mean square (rms). Figure 5 shows a picture of the mirror unit after assembly.

3.5 *On and Off Process*

As discussed in the previous section, the ASM should be able to provide scientifically useful images even when in power-off mode. This also requires the mirror to be disturbed as little as possible during the switch-off process. Simply turning off the mirror was found to leave distortions depending on the positions of the actuators because of their hysteresis. Therefore, a controlled switch-off method was required to overcome the residual hysteresis problem.

The controlled switch-off method can be summarized as the following:

1. During the assembly, all the actuators were zero positioned on the hysteresis curve by applying a sinusoidal voltage that slowly decayed to zero.
2. In service, the actuators were switched off by applying decaying sinusoidal signals from the drive electronics. In case of the control system failure, the process can be done by an independent hard-wired backup system powered from a rechargeable battery.

The effectiveness of the technique was tested by switching off the mirror, powering it up and cycling the actuators, then switching off again. Following the preceding procedure the initial and final interferograms were compared and revealed an optical path difference (OPD) of 77 nm rms, corresponding to a change of 38 nm rms in the mirror shape.

4 Static Testing

The influence functions of the demonstrator were measured by comparing the OPDs before and after movement. The OPDs were measured by a phase-shift interferometer from WYKO Corporation, Tucson, Arizona (a WYKO 6000). Since the interferometer can not measure the piston effect of OPD, independent measurements using an eddy current sensor were carried out. Figure 6 shows the measured influence functions of the central and one outer actuator. The influence functions were normalized to have a maximum displacement of 1 μm. Comparison of the measured influence functions with the FEA-derived ones (Fig. 7) shows excellent correspondence.

The demonstrator was then deformed to match the low order Zernike polynomial terms. The control signals were derived as described in Ref. 9. Because of nonlinearity (hysteresis and thermal expansion) of the prototype actuators and electrical noise in the displacement sensors, the actuator control signals required to match the Zernike terms were slightly different from those calculated using the measured influence functions. To correct for this the actuator voltages were tuned to match the exact theoretical Zernike deformation by reference to the interferograms measured by the WYKO. The rms residual errors were reduced to 35 nm. Figure 8 shows the measured mirror deformation optimized to match the Zernike terms (two tilt defocus, astigmatism), and the residual errors for these terms are shown in Fig. 9. More accurate fitting can be achieved if the residual nonlinearity of the actuators is reduced or compensated for, or if the system were operated with feedback from a wavefront sensing camera.

The demonstrator was predicted[9] by FEA to provide near-perfect tip/tilt, defocus and astigmatism and the experimental results confirmed this prediction. Unlike conventional tip/tilt mirrors, the tip/tilt motion of the demonstrator is not a pure rigid body motion due to the

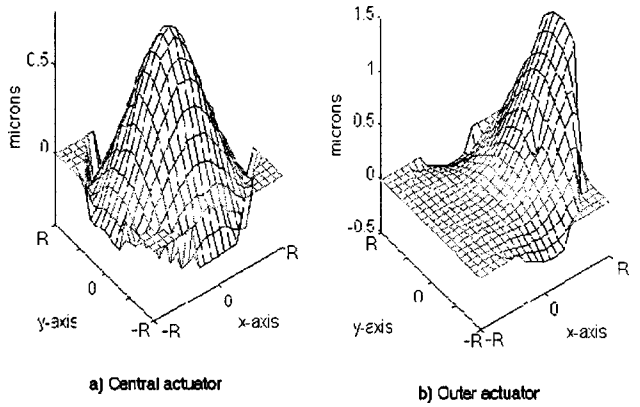

Fig. 7 FEA-derived influence functions of the central and outer actuators with a stroke of 1 Om respectively, and *R* is the radius of the mirror.

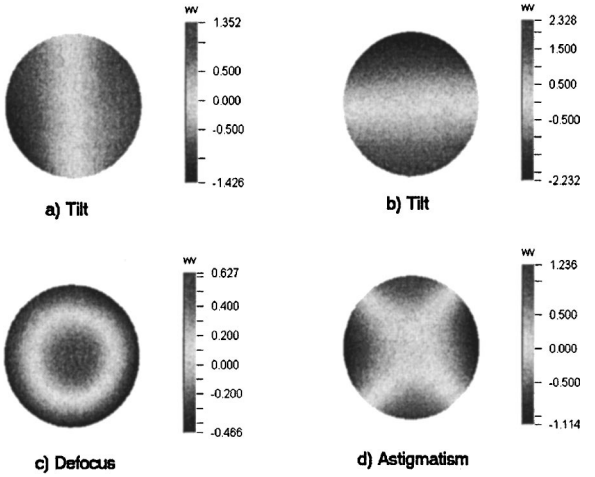

Fig. 8 Measured mirror deformation to match the first four Zernike terms: two tilts, defocus, and astigmatism.

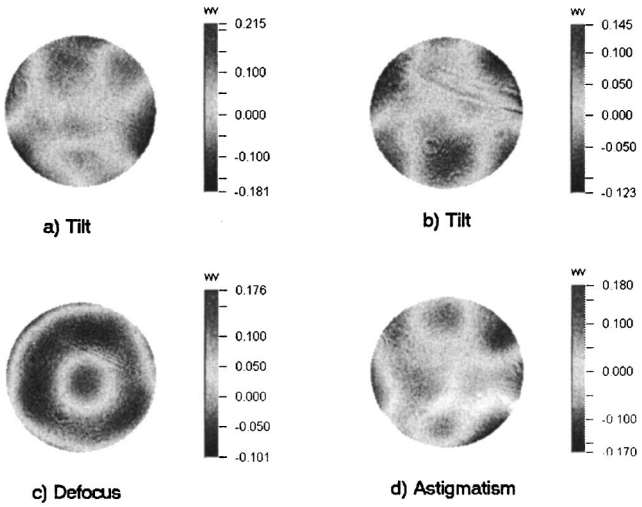

Fig. 9 Measured residual errors of the mirror deformation matching the Zernike terms: two tilts, defocus, and astigmatism.

mechanical moment caused by the flexure joints in the actuator connections to the mirror substrate. Note that the tip/tilt component is responsible for 87% of the total atmospheric variance so removing tip/tilt well is a fundamental requirement for the demonstrator. The importance, therefore, of the experimental proof that the demonstrator can perform almost perfect tip/tilt can not be over emphasized.

5 Dynamic Testing

Before carrying out a dynamic test of the mirror, a separate analysis and experiments were performed to estimate and test the performance of the positioning system. These show that the positioning system a dynamic cut-off frequency of 60 Hz, which is 12 times higher than the typical Greenwood frequency ($\approx$5 Hz) of the adaptive optics (AO) operation in the IR waveband (2.2 μm). Together with the results of the simulation and experiments of the static performance, the results of positioning system tests show that the demonstrator is capable of correcting time-varying tip/tilt aberration at least up to the cut off frequency.

As a preliminary experiment the demonstrator was operated in a closed-loop with a quad cell detector. The optical layout for the dynamic experiment (Fig. 10) is the same as for the static test except that a beamsplitter was added as a pick-off for the quad cell. The interferometer is out of the loop but provides a reference measurement of the mirror deformation. Periodic tip/tilt wavefront errors (0.73 Hz) were introduced by rotating an inclined sheet of window glass in the laser optical beam.

Figures 11 and 12 show the tip/tilt signals from the quad cell when tip/tilt wavefront aberrations were introduced and demonstrator system was respectively open and closed via the quad cell detector. Calibration of the quad cell signal was done using the interferometer.

These two figures clearly show that the demonstrator is capable of compensating a time-varying tip/tilt wavefront. The amplitude of periodic tip/tilt aberrations was suppressed from 2 to 0.2 arcsec. During experimentation, residual hysteresis was found in the actuators at levels of 2% and 8% for a cycle of amplitude of $\sim$9 and 25 μm. This is believed to be due to incorrect bonding of the strain gauge to the actuator, which will be remedied in the next generation of actuators. Furthermore, the prototype actuators had only a single strain gauge, which will be replaced with a bridge configuration to provide thermal compensation.

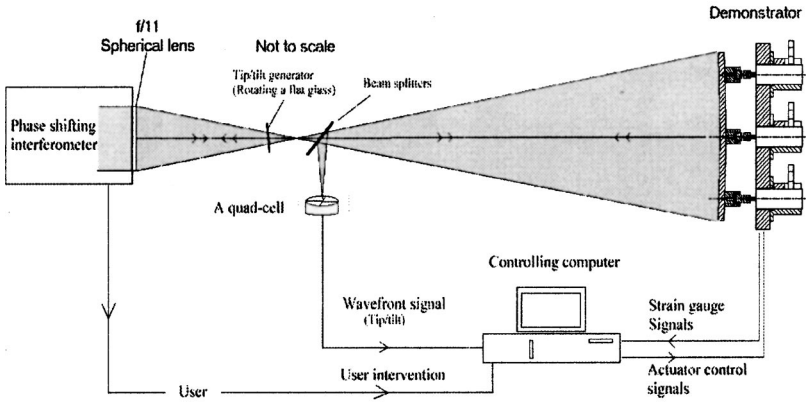

Fig. 10 Optical setup for dynamic evaluation of the demonstrator.

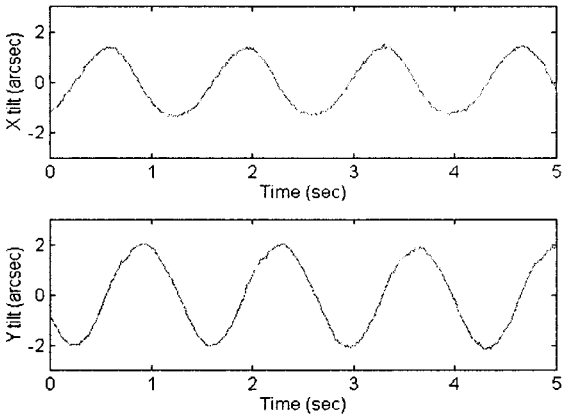

Fig. 11 Tip/tilt signals from the quad cell when tip/tilt wavefront aberrations were introduced by rotating the glass and the demonstrator system was in open loop operation.

6 Conclusion

The application of aluminum mirror technology is a primary feature of the demonstrator. This is one of the first AO systems to use a metal mirror as a deformable wavefront corrector. The ability to preserve the optical quality of the aluminum mirror during assembly and to deform the mirror shape as required are fundamental requirements of adaptive secondaries. To that end error-free assembly techniques were developed and successfully implemented resulting in the errors in the mirror shape of less than 10 nm rms. The ability of the metal mirror to fit lower order Zernike terms was initially predicted[9] in simulation using FEA and was later confirmed by laboratory tests.

These successful results open the possibility of future adaptive optics systems using this metal mirror technology. An attractive application of this outside astronomy is the compensation of self-induced free-air turbulent in very high power laser systems, where the adaptive metal mirror lends itself ideally to liquid cooling.

The demonstrator is planned to be tested on the optical bench in the Ground-based High Imaging Laboratory (GHRIL) at the William Herschel Telescope (WHT) to investigate ASM performance under real seeing conditions.

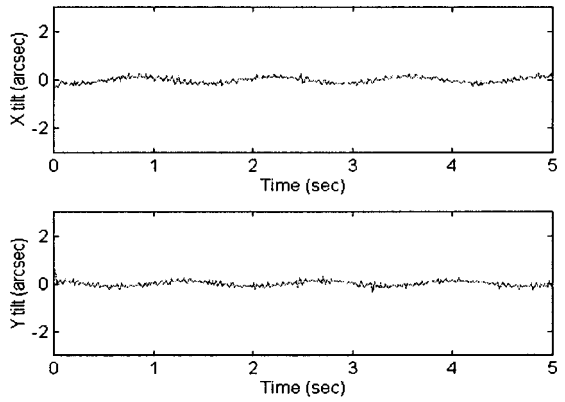

Fig. 12 Tip/tilt signals from the quad cell when tip/tilt wavefront aberrations were introduced by rotating the glass and the demonstrator system was in closed loop operation.

To achieve this, the faceplate is going to be refigured/polished and the demonstrator is tested with a fast wavefront sensor.

Acknowledgments

The work described in this paper was financed from a number of sources, including the Satellite Technology Research Center (SaTReC) of the Korea Advanced Institute of Science and Technology (KAIST), the United Kingdom Gemini project office, and the United Kingdom Particle Physics and Astronomy Research Council.

References

1. J. M. Beckers, ''Adaptive optics for astronomy: principles, performance, and applications,'' *Annu. Rev. Astron. Astrophys.* **31**, 13–62 (1993).
2. J. M. Beckers, ''A proposal to the National Science Foundation,'' in the *NOAO 8-M Telescope Technical Digest*, Vol. II, Association for University Research in Astronomy (1989).
3. L. M. Close and D. W. McCarthy, ''High-resolution imaging with a tip/tilt cassegrain secondary,'' *Publ. Astron. Soc. Pac.* **106**, 77–86 (1994).
4. E. Pitz, R. R. Rohloff, and H. Marth, ''UKIRT 5-axis tip/tilt secondary electro-mechanical and optical design,'' *Proc. ESO* , (1993).
5. P. Salinari and D. G. Sandler, ''High order adaptive secondary mirrors: Where are we?'' *Proc. SPIE* **3353**, 742–753 (1998).
6. D. D. Walker, R. G. Bingham, and B. C. Bigelow, ''Adaptive correction at telescope secondary mirrors,'' *Proc. ESO* **48**, 255–260 (1993).
7. B. C. Bigelow, D. D. Walker, R. G. Bingham, and P. D'Arrigo, ''A deformable secondary mirror for adaptive optics,'' *Proc. ESO* **48**, 261–266 (1993).
8. D. D. Walker, J. H. Lee, R. G. Bingham, D. Brooks, M. Dryburgh, G. Nixon, H. Jamshidi, S. W. Kim, and B. Bigelow, ''Rugged adaptive telescope secondaries: experience with a demonstrator mirror,'' *Proc. SPIE* **3353**, 872–877 (1998).
9. J. H. Lee, D. D. Walker, and A. P. Doel, ''Adaptive secondary mirror demonstrator: design and simulation,'' *Opt. Eng.* **38**(9), 1456–1461 (1999).
10. B. C. Bigelow, D. D. Walker, and G. Nixon, ''Testing of a magnetostrictive actuator for adaptive secondary mirror,'' *Proc. SPIE* **2871**, 910–919 (1996).

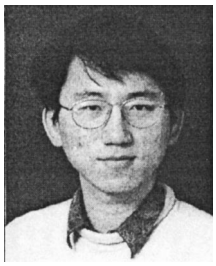

Jun Ho Lee received his BSc degree from the Mechanical Engineering Department of the Korea Advanced Institute of Science and Technology (KAIST) in 1994, his MSc degree with distinction in satellite communication and spacecraft technologies from University College London (UCL) in 1995, and his PhD in adaptive optics from UCL in 1999. During his PhD studies he was also involved in the development of a spaceborne camera. He is now a senior researcher in earth observation payload development division at the Satellite Technology Research Center, KAIST. His current research interests include space optics and adaptive optics for astronomical and industrial uses.

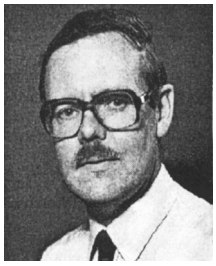

David D. Walker received his PhD in astronomical instrumentation for ground based telescopes from the University College London (UCL) in 1980. He subsequently developed cryogenic CCD cameras, and then led the development of the UCL Echelle Spectrograph for the Anglo Australian Telescope. In 1985 he was the founding director of the Optical Science Laboratory at UCL, which he still directs. He has led numerous other instrumentation projects and is currently the principal scientist for the Gemini High Resolution Optical Spectrograph. His research interests are focused on systems-level optimization of instrumentation applied over a broad range of applications, in particular adaptive optics, optical pro-

duction and metrology. He is also a founding director of a spin-off company Optical Generics Ltd., which is producing commercial machines for grinding and polishing aspheric optics.

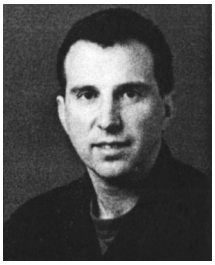

A. Peter Doel received his PhD in adaptive optics for large ground-based telescopes from the University of Durham in 1990 and joined the Astronomical Instrumentation Group in Durham as a postdoctural research assistant where he worked on the MARTINI, ELECTRA, and NAOMI adaptive optics systems for the 4.2 m William Herschel Telescope on La Palma, Canaries. In 1998 he took up a lectureship at the Optical Science Laboratory at University College London, where he heads the adaptive optics division. His research interests include atmospheric turbulence modeling and adaptive optics for astronomical and industrial uses.